Progress In Electromagnetics Research, PIER 21, 1–19, 1999

APPLICATION OF MULTI-DOMAIN GDQ METHOD TO ANALYSIS OF WAVEGUIDES WITH RECTANGULAR BOUNDARIES

C. Shu and Y. T. Chew

Department of Mechanical and Production Engineering
National University of Singapore
10 Kent Ridge Crescent
Singapore 119260

1. Introduction
2. Multi-Domain GDQ Approach
2.1 GDQ Formulation
2.2 Multi-Domain Approach
3. Formulation and Numerical Algorithms
4. Results and Discussion
4.1 Rectangular Waveguide
4.2 Double-Ridged Waveguide
4.3 L-Shaped Waveguide
4.4 Single-ridged Waveguide
4.5 Coaxial Rectangular Waveguide
4.6 Vaned Rectangular Waveguide
5. Conclusions
References

1. INTRODUCTION

The rectangular hollow conducting waveguides and many of their variations are widely used in microwave systems. The computation of the cutoff wavenumbers of these waveguides is one of important issues for designing the waveguide or analyzing the wave propagation in the waveguide. There are a variety of methods available in the literature to calculate the cutoff wavenumbers. Among them, the finite difference,

finite element and integral methods are used extensively. The early work has been summarized in [1]. More recently, the same problems have been studied by Swaminathan et al. [2] using the surface integral equation method, Sarkar et al [3], Guan and Su [4] using the finite difference method.

As we know, the finite difference and finite element methods are low order methods. To obtain accurate numerical results, these low order methods need to use a large number of grid points. Usually, the number of interior grid points for the cross section of a waveguide is equal to the dimension of the resultant eigenvalue equation system, and then provides the same number of cutoff wavenumbers. Among all the computed cutoff wavenumbers, only low cutoff wavenumbers are of practically interest. However, since all the computed cutoff wavenumbers have the same order of accuracy, one still needs to use a large number of grid points to obtain the better accuracy of such low cutoff wavenumbers. As a result, a lot of virtual storage and computational effort are required.

As will be shown in this paper, the global method of generalized differential quadrature (GDQ) offers a promising way for the analysis of waveguides. The accurate cutoff wavenumbers can be obtained by using a considerably small number of grid points. GDQ method was developed by Shu et al [5, 7] to improve the differential quadrature (DQ) method [6] in computing the weighting coefficients. It is indicated that GDQ is a global method which is based on the high order polynomial approximation. So far, the GDQ method has been efficiently applied to solve the fluid flow problems [7–8] and structural and vibration problems [9–10]. As shown in [5], GDQ method is equivalent to the highest order finite difference scheme. Thus, like the low order finite difference schemes, it requires the computational domain to be rectangular. However, for the practical application, the geometry of the problem is usually very complex. To apply the GDQ method to solve complex problems, we need to use the grid generation technique and the multi-domain approach which are widely applied in the low order finite difference schemes. In this paper, the efficiency and high accuracy of GDQ method is demonstrated by its application to a single-domain rectangular waveguide. Then a multi-domain GDQ approach is proposed. This approach divides the whole computational domain into several sub-domains. And in each subdomain, the GDQ method is used to discretize the derivatives. Globally, the information exchange

is conducted through the interface of neighboring subdomains. An overlapped interface topology will be used in this study.

2. MULTI-DOMAIN GDQ APPROACH

2.1 GDQ Formulation

GDQ approach was developed by Shu et al. [5, 7] to improve the differential quadrature (DQ) technique [6]. It approximates the spatial derivative of a function with respect to a space coordinate at a given grid point as a weighted linear sum of all the functional values at all grid points in the whole domain of that space coordinate. The computation of weighting coefficients by GDQ is based on the analysis of a high order polynomial approximation and the analysis of a linear vector space. The weighting coefficients of the first order derivative are calculated by a simple algebraic formulation, and the weighting coefficients of the second and higher order derivatives are given by a recurrence relationship. It has been shown by Shu [5] that GDQ approach is equivalent to the highest order finite difference scheme. The details of GDQ method can be found in [5, 7]. Some two-dimensional results are described as follows. For a smooth function $f(x, y)$, GDQ discretizes its nth order derivative with respect to x, and the mth order derivative with respect to y, at the grid point (x_i, y_j) as

$$f_x^{(n)}(x_i, y_j) = \sum_{k=1}^{N} c_{ik}^{(n)} \cdot f(x_k, y_j), n = 1, 2, \ldots, N-1 \tag{1a}$$

$$f_y^{(m)}(x_i, y_j) = \sum_{k=1}^{M} \overline{c}_{jk}^{(m)} \cdot f(x_i, y_k), m = 1, 2, \ldots, M-1 \tag{1b}$$

$$\text{for } i = 1, 2, \ldots, N;\ j = 1, 2, \ldots, M,$$

where N, M are the number of grid points in the x and y direction respectively, $c_{ik}^{(n)}, \overline{c}_{jk}^{(m)}$ are the weighting coefficients to be determined as follows,

weighting coefficients for the first order derivative

$$c_{ij}^{(1)} = \begin{cases} \dfrac{A^{(1)}(x_i)}{(x_i - x_j) \cdot A^{(1)}(x_j)}, & \text{when } j \neq i \\ \displaystyle\sum_{k=1, k\neq i}^{N} c_{ik}^{(1)}, & \text{when } j = i \end{cases} \tag{2a}$$

$$\text{for } i,j = 1,2,\ldots,N,$$

$$\overline{c}_{ij}^{(1)} = \begin{cases} \dfrac{B^{(1)}(y_i)}{(y_i - y_j)\cdot B^{(1)}(y_j)}, & when\ j \neq i \\ \displaystyle\sum_{k=1,k\neq i}^{M} \overline{c}_{ik}^{(1)}, & when\ j = i \end{cases} \tag{2b}$$

$$\text{for } i,j = 1,2,\ldots,M,$$

where

$$A^{(1)}(x_i) = \prod_{j=1,j\neq i}^{N} (x_i - x_j),$$

$$B^{(1)}(y_i) = \prod_{j=1,j\neq i}^{M} (y_i - y_j).$$

weighting coefficients for the second and higher order derivatives

$$c_{ij}^{(n)} = \begin{cases} n\cdot\left(c_{ii}^{(n-1)}\cdot c_{ij}^{(1)} - \dfrac{c_{ij}^{(n-1)}}{x_i - x_j}\right), & when\ j \neq i \\ \displaystyle\sum_{k=1,k\neq i}^{N} c_{ik}^{(n)}, & when\ j = i \end{cases} \tag{3a}$$

$$\text{for } i,j = 1,2,\ldots,N, n = 2,3,\ldots,N-1,$$

$$\overline{c}_{ij}^{(m)} = \begin{cases} m\cdot\left(\overline{c}_{ii}^{(m-1)}\cdot \overline{c}_{ij}^{(1)} - \dfrac{\overline{c}_{ij}^{(m-1)}}{y_i - y_j}\right), & when\ j \neq i \\ \displaystyle\sum_{k=1,k\neq i}^{M} \overline{c}_{ik}^{(m)}, & when\ j = i \end{cases} \tag{3b}$$

$$\text{for } i,j = 1,2,\ldots,M, m = 2,3,\ldots,M-1,$$

It is obvious from above formulations that the weighting coefficients of the second and higher order derivatives can be completely determined from those of the first order derivatives. When the coordinates of grid points are known, the weighting coefficients for the discretization of derivatives can be easily calculated from formulations (2), (3). Then using equation (1), all the spatial derivatives can be discretized using

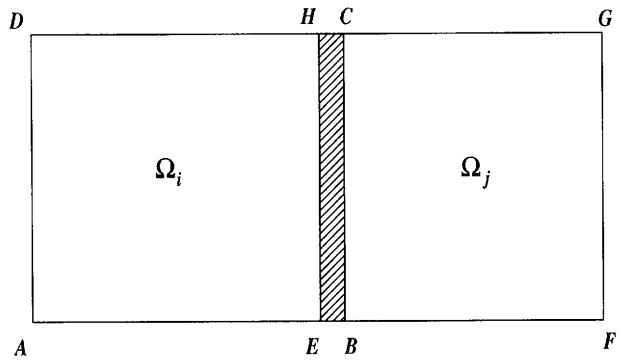

Figure 1. Topology of two overlapped subdomains.

a similar form. The difference for the respective derivatives is to use different weighting coefficients, which are usually computed in advance. This avails as an easily implementable scheme on the computer with greatly simplified code-editing features.

2.2 Multi-Domain Approach

Like the conventional low order finite difference schemes, GDQ approach requires the computational domain to be rectangular. However, in practical applications, the physical domain is usually complex. For this case, the GDQ approach cannot be applied directly. This difficulty can be removed by the choice of grid generation and multi-domain technique. In the following, a multi-domain GDQ approach is presented.

The multi-domain GDQ approach, firstly, decomposes the whole computational domain into several subdomains. Then in each subdomain, a local mesh is generated and a local GDQ technique is applied in the same fashion as the application of GDQ in a single domain. Globally, the information exchange between neighboring subdomains is conducted through the interface. Since any complex geometry can be transformed into a rectangular domain or a combination of rectangular subdomains, a rectangular domain is chosen for demonstration without losing generality. As shown in Fig. 1, in this study, the two neighboring subdomains are overlapped by one mesh point. The subdomain ABCD is overlapped with the subdomain EFGH (shaded area).

It is noted that the right boundary of the subdomain Ω_i, BC, is in the interior of the subdomain Ω_j, and the left boundary of the subdomain Ω_j, EH, is in the interior of the subdomain Ω_i. Obviously, the information between the two subdomains Ω_i and Ω_j is exchanged through the boundaries BC and EH. In each subdomain, the governing equation is discretized at all interior points. Since the boundary of a subdomain is in the interior of another subdomain, so, globally, the governing equation is discretized in the interior of whole computational domain.

3. FORMULATION AND NUMERICAL ALGORITHMS

It is well known that the propagation characteristics of the hollow conducting waveguides with homogeneous permittivity and permeability distributions can be fully determined by the following Helmholtz equation

$$\nabla^2\phi + k_c^2\phi = 0 \quad \text{in } \Omega \tag{4}$$

where k_c is the cutoff wavenumber, ϕ is the longitudinal component of electric or magnetic field defined in the two-dimensional domain Ω surrounded by the boundary Γ, ∇^2 is the Laplacian operator given by

$$\nabla^2 = \frac{\partial^2}{\partial x^2} + \frac{\partial^2}{\partial y^2}$$

The corresponding boundary conditions are the Dirichlet and Neumann conditions at Γ for the guiding TM and TE modes. The boundary conditions for the TM modes are

$$\phi = 0 \quad \text{at } \Gamma \tag{5}$$

and the boundary conditions for the TE modes are

$$\frac{\partial\phi}{\partial n} = 0 \quad \text{at } \Gamma \tag{6}$$

For the application of multi-domain GDQ approach, the whole domain Ω is divided into K subdomains. Then in each subdomain $\Omega_k, k = 1, 2, \ldots, K$, the GDQ method is applied to discretize the derivatives in equation (4). It is supposed that in Ω_k there are N grid points in the x direction and M grid points in the y direction. The corresponding

weighting coefficients of the second order derivatives in the x and y directions are noted as $w_{in}^{(2)}$, $\overline{w}_{jm}^{(2)}$ respectively.

Using GDQ method, equation (4) can be discretized as

$$\sum_{n=1}^{N} w_{in}^{(2)} \cdot \phi_{nj} + \sum_{m=1}^{M} \overline{w}_{jm}^{(2)} \cdot \phi_{im} = -k_c^2 \phi_{ij} \quad \text{in } \Omega_k \tag{7}$$

Similarly, the derivative in the Neumann boundary condition can be discretized by GDQ method. After numerical discretization, the Dirichlet or Neumann boundary condition can be directly substituted into equation (7). Applying equation (7) in all the subdomains results in the following eigenvalue equation system

$$[A] \cdot \{\phi\} = -k_c^2 \{\phi\} \tag{8}$$

For a general case, [A] is considered as a full matrix. From equation (8), the k_c values (cutoff wavenumbers) can be obtained from the eigenvalues of matrix [A]. In this study, the eigenvalues of matrix [A] are obtained by using HQR subroutine provided by "Numerical Recipes".

4. RESULTS AND DISCUSSION

The efficiency of GDQ method is first studied by its application to the rectangular waveguides. For this case, the GDQ method is applied in the whole computational domain, and the GDQ results are compared with the analytical solution. Then the multi-domain GDQ approach is applied to compute the cutoff wavenumbers of the TM and TE modes for the L-shaped, single-ridged, double-ridged, coaxial rectangular, and vaned rectangular waveguides. The multi-domain GDQ results are compared with available data in the literature. It is noted that for all the cases, when the TE modes are considered, there is a null mode with the cutoff wavenumber being equal to zero in the computed GDQ results. However, this null mode does not exist physically and is removed from the corresponding tables. It was also found that when the same mesh size is used, the computation time required for TE modes is almost the same as that for TM modes.

4.1 Rectangular Waveguide

Consider a rectangular waveguide with length $a = 4.0\,\text{cm}$ and width $b = 3.0\,\text{cm}$ as shown in Fig. 2. The cutoff wavenumbers of the TE

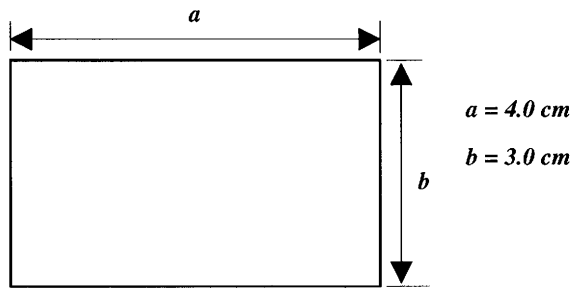

Figure 2. Configuration of a rectangular waveguide.

modes will be computed by GDQ and then compared with exact solution. For the TE modes, the Neumann condition should be applied at all the boundaries and the analytical solution can be expressed by

$$k_c = \pi\sqrt{(m/a)^2 + (n/b)^2}, \quad m, n = 0, 1, 2, \ldots \tag{9}$$

For the GDQ computation, the following mesh point distribution [7] is applied,

$$x_i = \frac{1}{2}\left[1 - \cos\left(\frac{i-1}{N-1}\cdot\pi\right)\right]a, \quad i = 1, 2, \ldots, N, \tag{10a}$$

$$y_j = \frac{1}{2}\left[1 - \cos\left(\frac{j-1}{M-1}\cdot\pi\right)\right]b, \quad j = 1, 2, \ldots, M \tag{10b}$$

where x_i, y_j represent the coordinates of mesh points. Table 1 shows the computed GDQ cutoff wavenumbers of the first ten TE modes and the corresponding absolute errors. Two mesh sizes of 9×9 and 15×15 are used to obtain GDQ results. The analytical solution is also included in Table 1 for comparison. It is observed that the coarse mesh of 9×9 provides the reasonable GDQ results, and as the mesh size is increased to 15×15, the accuracy of GDQ results is greatly improved. This shows that GDQ is a very efficient numerical method with high accuracy. Apart from the high order accuracy of GDQ results, the required computational effort is also tiny. For the results shown in Table 1, the computation time required on LEONIS is less than 1 second for each case.

In the following, the multi-domain GDQ results are presented for various waveguides. The TE and TM modes are followed by an integer subscript in ascending order of the cutoff wavenumbers, and the mesh sizes indicated in Tables 2–6 represent the mesh sizes in each subdomain.

Analytical Solution	Single-Domain GDQ Results		Absolute Errors	
	Mesh Sizes		*Mesh Sizes*	
	9×9	15×15	9×9	15×15
0.785398185	0.785394884	0.785398163	3.30115×10^{-6}	2.18552×10^{-8}
1.047197580	1.047193179	1.047197551	4.40153×10^{-6}	2.91405×10^{-8}
1.308996975	1.308991474	1.308996939	5.50191×10^{-6}	3.64255×10^{-8}
1.570796371	1.570512100	1.570796328	2.84270×10^{-4}	4.24891×10^{-8}
1.887862286	1.887623324	1.887862234	2.38962×10^{-4}	5.15173×10^{-8}
2.094395161	2.094016134	2.094395104	3.79027×10^{-4}	5.66520×10^{-8}
2.236815012	2.236458963	2.236814951	3.56049×10^{-4}	6.07189×10^{-8}
2.356194556	2.367932913	2.356193286	1.17384×10^{-2}	1.27011×10^{-6}
2.578425015	2.589154270	2.578423842	1.07293×10^{-2}	1.17248×10^{-6}
2.617993951	2.617520167	2.617993880	4.73783×10^{-4}	7.08151×10^{-8}

Table 1. Analytical and single-domain GDQ results of a rectangular waveguide.

4.2 Double-Ridged Waveguide

The first example for the application of multi-domain GDQ approach is the analysis of a double ridged waveguide. For this problem, the cutoff wavenumbers of the TE_1, TE_3, TE_5, TE_7 and TE_9 modes computed by various methods are available in the literature [4, 11–13]. The configuration of a double-ridged waveguide with $a = 1.27\,\text{cm}$, $b = 1.016\,\text{cm}$, $c = 0.508\,\text{cm}$, $d = 0.3683\,\text{cm}$ and the distribution of subdomains for the multi-domain GDQ computation are shown in Fig. 3. Seven subdomains are used for this problem. Table 2 displays the cutoff wavenumbers of the TE_1, TE_3, TE_5, TE_7 and TE_9 modes for a double-ridged waveguide computed by the multi-domain GDQ approach and other approaches [4, 11–13]. In Table 2, the multi-domain GDQ results are given by using five different

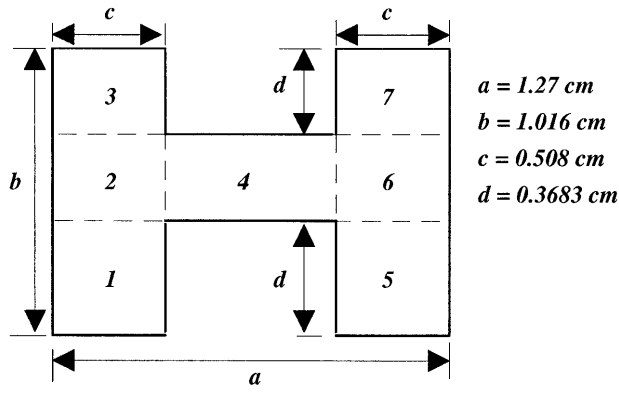

Figure 3. Configuration of a double ridged waveguide and distribution of subdomains.

Approaches	*Meshes*	TE_1	TE_3	TE_5	TE_7	TE_9
Multi-domain GDQ	7×7	1.4302	3.1645	6.1911	6.7030	6.9760
	9×9	1.4398	3.1677	6.1913	6.7092	6.9757
	11×11	1.4423	3.1685	6.1915	6.7116	6.9761
	15×15	1.4428	3.1686	6.1917	6.7127	6.9760
	19×19	1.4423	3.1684	6.1917	6.7127	6.9757
FD-SIC [4]	50×40	1.428	3.169	6.192	6.695	6.976
	100×80	1.434	3.168	6.192	6.705	6.975
Montgomery [11]		1.437	3.166	6.190	6.712	6.973
Utsumi [12]		1.438	3.155	6.215	6.707	6.971
Scalar-FEM [13]		1.440	-	6.192	6.713	-

Table 2. Comparison of cutoff wavenumbers for a double-ridged waveguide.

mesh sizes, and the results of the finite difference and simultaneous iteration with Chebyshev acceleration (FD-SIC) method [4] are given from two different mesh sizes. It should be indicated that the mesh size for the FD-SIC solution represents the mesh size for one quarter of the waveguide cross section. It can be observed from the table that the multi-domain GDQ approach is very efficient. When a very coarse mesh of 7×7 is used in each subdomain, the multi-domain

GDQ results are very accurate, and the required computation time on LEONIS is just 2 seconds. As the mesh is refined, the multi-domain GDQ results are converged to a grid-independent solution. Although the multi-domain GDQ results are in good agreement with all the data available in the literature, they are more close to the results of FD-SIC [4] and scalar-FEM [13]. This can be seen clearly in Table 2.

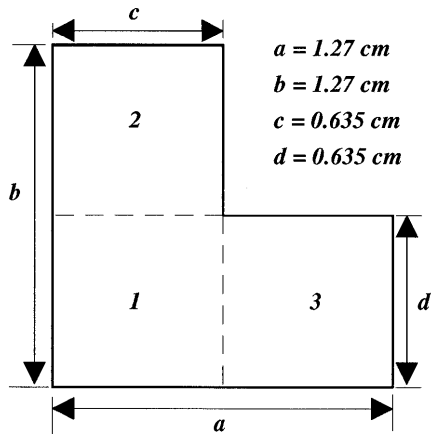

Figure 4. Configuration of a L-shaped waveguide and distribution of subdomains.

4.3 L-Shaped Waveguide

The configuration of a L-shaped waveguide with $a = b = 1.27\,\text{cm}$, $c = d = a/2$ and the distribution of subdomains are shown in Fig. 4. Three subdomains are used for this problem. In each subdomain, the same mesh size is used. Table 3 shows the computed cutoff wavenumbers of the first ten TM and TE modes by multi-domain GDQ approach for a L-shaped waveguide. Also included in this table are the results of the surface integral equation (SIE) method [2], the finite difference with conjugate gradient method (FD-CGM) [3], and the FD-SIC method [4]. The multi-domain GDQ results are obtained by using four different mesh sizes. It can be seen from the table that the convergence of multi-domain GDQ results is very good, and the present results agree very well with the results of FD-SIC [4] which are based on a mesh size of 50×50. As shown in [4], analytical solutions

	Multi-Domain GDQ				FD-SIC	FD-CGM	SIE
Meshes	9×9	13×13	17×17	21×21	[4]	[3]	[2]
TM Modes							
TM_1	4.8976	4.8922	4.8907	4.8902	4.8949	4.80	4.8677
TM_2	6.1390	6.1391	6.1392	6.1392	6.1350	6.07	6.1361
TM_3	6.9967	6.9967	6.9967	6.9967	6.9921	6.92	6.9908
TM_4	8.5565	8.5565	8.5565	8.5565	8.5458	8.61	8.5525
TM_5	8.9073	8.9000	8.8980	8.8972	8.8940	9.72	-
TM_6	10.1493	10.1443	10.1430	10.1425	10.1262	11.39	-
TM_7	10.5577	10.5580	10.5580	10.5580	10.5318	-	-
TM_8	11.0628	11.0627	11.0627	11.0627	11.0380	-	-
TM_9	11.0628	11.0627	11.0627	11.0627	11.0380	-	-
TM_{10}	11.8663	11.8615	11.8603	11.8598	11.8407	-	-
TE Modes							
TE_1	1.9053	1.9104	1.9118	1.9123	1.9111	-	1.8917
TE_2	2.9604	2.9605	2.9605	2.9605	2.9600	-	2.9159
TE_3	4.9474	4.9474	4.9474	4.9474	4.9452	-	4.8755
TE_4	4.9474	4.9474	4.9474	4.9474	4.9452	-	-
TE_5	5.3147	5.3147	5.3147	5.3147	5.3128	-	5.2463
TE_6	5.5752	5.5810	5.5825	5.5831	5.5799	-	-
TE_7	6.9967	6.9967	6.9967	6.9967	6.9937	-	-
TE_8	7.2736	7.2840	7.2868	7.2879	7.2784	-	-
TE_9	7.6085	7.6088	7.6088	7.6088	7.6002	-	-
TE_{10}	8.3912	8.4009	8.4035	8.4045	-	-	-

Table 3. Cutoff wavenumbers of a L-shaped waveguide.

of this problem for TM_3, TM_8, TM_9, TE_3, TE_4, TE_7 modes are available. Their respective values are 6.9967, 11.0627, 11.0627, 4.9474, 4.9474, and 6.9967. Table 3 shows that when the mesh size in each subdomain is taken as 13×13, the multi-domain GDQ results match the analytical solution of above modes up to four decimal digits. Clearly, as the mesh is refined, the accuracy of multi-domain GDQ results is improved. From the convergence trend, it is believed that the multi-domain GDQ results with a mesh size of 9×9 are more accurate than the results of SIE [2], FD-CGM [3], and FD-SIC [4]. It was found that the calculated cutoff wavenumbers of TM_5 and TM_6 modes by the

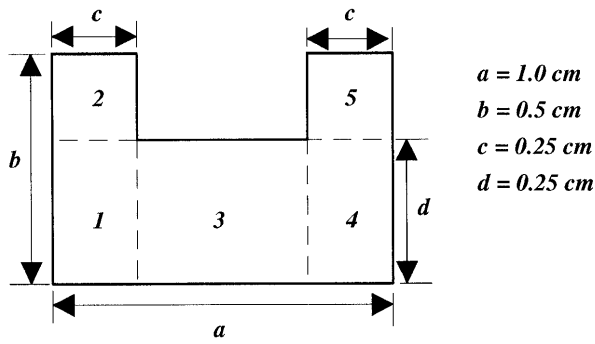

Figure 5. Configuration of a single ridged waveguide and distribution of subdomains.

FD-CGM are not close to any of our results for the modes from TM_1 to TM_{10}. This finding has also been discussed in [4]. When the mesh size of 9×9 is used, the required computation time on LEONIS is just 1 second.

4.4 Single-Ridged Waveguide

The configuration of a single-ridged waveguide with $a = 1.0\,\text{cm}$, $b = 0.5\,\text{cm}$, $c = d = 0.25\,\text{cm}$ and the distribution of subdomains are shown in Fig. 5. Five subdomains are used for this problem. Table 4 displays the computed cutoff wavenumbers of the first ten TM and TE modes for a single-ridged waveguide. In the table, the multi-domain GDQ results using four mesh sizes are compared with the results of SIE [2], FD-CGM [3], and FD-SIC [4]. It was found that the multi-domain GDQ results with a mesh size of 9×9 are very accurate. For this case, the computation time on LEONIS is just 2 seconds. As the mesh is refined, the accuracy of multi-domain GDQ results is improved. The present multi-domain GDQ results agree very well with the results of FD-SIC [4]. However, there are some discrepancies between the present results and the results of SIE [2] and FD-CGM [3]. For all the cases, the results of SIE [2] and FD-CGM [3] are smaller than our results. From the comparison in Table 4, it seems that the cutoff wavenumber of the TM_6 mode is lost in the FD-CGM computation.

	Multi-Domain GDQ				FD-SIC	FD-CGM	SIE
Meshes	9×9	13×13	17×17	21×21	[4]	[3]	[2]
TM Modes							
TM_1	12.1520	12.1406	12.1374	12.1362	12.1447	12.05	12.0381
TM_2	12.4399	12.4263	12.4225	12.4210	12.4331	12.32	12.2938
TM_3	14.0118	14.0098	14.0093	14.0090	14.0037	13.86	13.9964
TM_4	15.5931	15.5934	15.5935	15.5935	15.5829	15.34	15.5871
TM_5	16.6509	16.6508	16.6507	16.6507	16.6403	16.28	-
TM_6	17.7715	17.7715	17.7715	17.7715	17.7598	-	-
TM_7	19.6461	19.6451	19.6448	19.6447	19.6296	19.32	-
TM_8	21.7344	21.7335	21.7335	21.7335	21.7063	-	-
TM_9	22.2980	22.2878	22.2849	22.2838	-	-	-
TM_{10}	22.6256	22.6060	22.6010	22.5990	-	-	-
TE Modes							
TE_1	2.2427	2.2472	2.2484	2.2489	2.2422	2.23	2.2496
TE_2	4.8395	4.8524	4.8559	4.8573	4.8543	4.78	4.9436
TE_3	6.4441	6.4518	6.4540	6.4548	6.4476	6.40	6.5189
TE_4	7.5195	7.5196	7.5196	7.5196	7.5185	7.48	7.5642
TE_5	9.8222	9.8245	9.8252	9.8254	9.8314	9.71	-
TE_6	12.5663	12.5664	12.5664	12.5664	12.5607	12.39	-
TE_7	12.5663	12.5664	12.5664	12.5664	12.5607	-	-
TE_8	12.7761	12.7779	12.7783	12.7785	12.7667	-	-
TE_9	13.3771	13.3805	13.3814	13.3818	13.3825	-	-
TE_{10}	13.4992	13.4993	13.4993	13.4993	-	-	-

Table 4. Cutoff wavenumbers of a single-ridged waveguide.

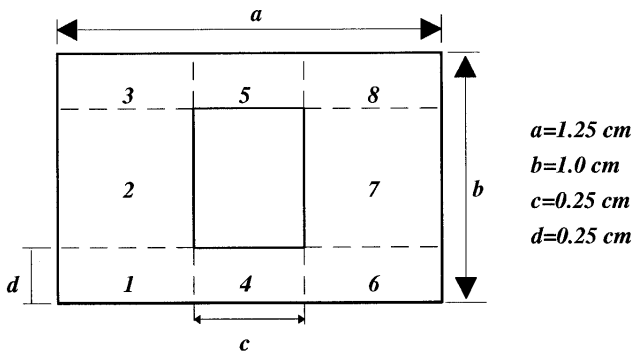

Figure 6. Configuration of a coaxial waveguide and distribution of subdomains.

4.5 Coaxial Rectangular Waveguide

The configuration of a coaxial rectangular waveguide with $a = 1.25\,\text{cm}$, $b = 1.0\,\text{cm}$, $c = 0.25\,\text{cm}$, $d = 0.25\,\text{cm}$ and the distribution of subdomains are shown in Fig. 6. Eight subdomains are used for this problem. Table 5 shows the computed cutoff wavenumbers of the first ten TM and TE modes by multi-domain GDQ approach for a coaxial rectangular waveguide. The multi-domain GDQ results are obtained by using six different mesh sizes, and are compared with the results of FD-CGM [3]. Obviously, the convergence of multi-domain GDQ results is excellent. As the number of mesh points is increased a little, the accuracy of GDQ results is improved a lot. From the convergence trend of GDQ results, it is believed that the multi-domain GDQ results with a mesh size of 7×7 are more accurate than the results of FD-CGM [3]. For the mesh size of 7×7, the required computation time on LEONIS is just 3 seconds.

4.6 Vaned Rectangular Waveguide

The configuration of a vaned rectangular waveguide with $a = 2.0\,\text{cm}$, $b = 1.0\,\text{cm}$, $c = 0.5\,\text{cm}$ and the distribution of subdomains are shown in Fig. 7. Four subdomains are used for this problem. Table 6 exhibits the computed cutoff wavenumbers of the first ten TM and TE modes for a vaned rectangular waveguide. In Table 6, the multi-domain GDQ results using five different mesh sizes are compared with the results of SIE [2] and FD-CGM [3]. Like other problems, the convergence of multi-domain GDQ results for this problem is also very good. As the mesh size is refined, the multi-domain GDQ results will converge to a grid-independent solution. It can be observed from Table 6 that for the TE modes, the present results agree well with the results of SIE [2] and FD-CGM [3]. For the TM modes, the present results also agree well with the results of SIE [2]. However, there are some significant discrepancies between the present results and the results of FD-CGM [3] for the TM modes. It can be seen from the table that calculated cutoff wavenumbers of the TM_4, TM_5 and TM_6 between the two results are quite different. It was found that the cutoff wavenumber of the TM_4 mode in the FD-CGM solution is close to the cutoff wavenumber of the TM_6, or TM_7 mode in the multi-domain GDQ solution, and the cutoff wavenumber of the TM_5 mode

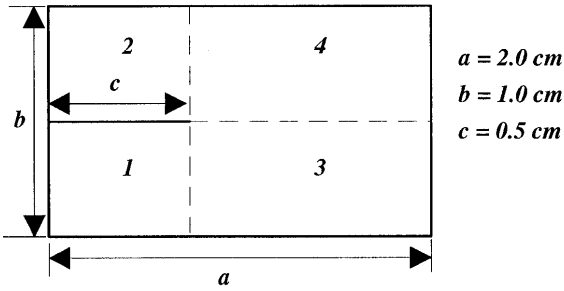

Figure 7. Configuration of a vaned rectangular waveguide and distribution of subdomains.

	Multi-Domain GDQ						FD-CGM
Meshes	7×7	9×9	11×11	13×13	15×15	17×17	[3]
TM Modes							
TM_1	6.9468	6.9422	6.9403	6.9395	6.9390	6.9387	6.91
TM_2	6.9569	6.9528	6.9512	6.9504	6.9499	6.9497	6.96
TM_3	8.6691	8.6590	8.6550	8.6531	8.6520	8.6514	8.50
TM_4	8.7080	8.6997	8.6963	8.6946	8.6938	8.6932	8.51
TM_5	10.9402	10.9275	10.9223	10.9197	10.9184	10.9176	10.57
TM_6	11.0709	11.0628	11.0594	11.0578	11.0569	11.0564	10.83
TM_7	12.5439	12.5199	12.5090	12.5039	12.5011	12.4994	-
TM_8	12.5513	12.5370	12.5307	12.5278	12.5263	12.5253	-
TM_9	12.7408	12.7286	12.7238	12.7216	12.7205	12.7198	-
TM_{10}	13.2120	13.1917	13.1820	13.1775	13.1751	13.1737	-
TE Modes							
TE_1	1.8829	1.8893	1.8907	1.8908	1.8904	1.8900	1.85
TE_2	2.7913	2.8099	2.8185	2.8232	2.8261	2.8281	2.81
TE_3	3.9041	3.9086	3.9100	3.9105	3.9107	3.9108	3.89
TE_4	5.0850	5.1140	5.1269	5.1339	5.1381	5.1410	5.05
TE_5	5.7158	5.7339	5.7422	5.7468	5.7497	5.7516	5.68
TE_6	6.3520	6.3539	6.3545	6.3545	6.3544	6.3543	6.25
TE_7	6.3597	6.3613	6.3617	6.3616	6.3614	6.3612	-
TE_8	7.0409	7.0434	7.0447	7.0450	7.0451	7.0451	-
TE_9	7.8921	7.8975	7.8999	7.9007	7.9010	7.9010	-
TE_{10}	8.1344	8.1562	8.1657	8.1702	8.1726	8.1740	-

Table 5. Cutoff wavenumbers of a coaxial rectangular waveguide.

	Multi-Domain GDQ					FD-CGM	SIE
Meshes	7×7	11×11	15×15	19×19	23×23	[3]	[2]
TM Modes							
TM_1	3.7093	3.6984	3.6952	3.6939	3.6932	3.65	3.6770
TM_2	5.0180	4.9873	4.9783	4.9745	4.9726	4.87	4.9279
TM_3	6.4747	6.4766	6.4766	6.4747	6.4721	6.31	6.4151
TM_4	6.4766	6.4924	6.4798	6.4766	6.4766	7.59	-
TM_5	7.0243	7.0248	7.0248	7.0248	7.0248	8.65	7.0220
TM_6	7.7225	7.7475	7.7444	7.7433	7.7428	9.29	-
TM_7	7.8591	7.8540	7.8540	7.8540	7.8540	-	-
TM_8	8.7780	8.8857	8.8858	8.8841	8.8831	-	-
TM_9	9.6309	8.8935	8.8860	8.8858	8.8858	-	-
TM_{10}	9.8524	9.6341	9.6333	9.6329	9.6328	-	-
TE Modes							
TE_1	1.5582	1.5660	1.5683	1.5693	1.5698	1.57	1.5695
TE_2	1.9133	2.0247	2.0585	2.0730	2.0805	2.0	2.1156
TE_3	3.1107	3.1293	3.1353	3.1378	3.1390	3.13	3.1568
TE_4	3.3034	3.3034	3.3035	3.3036	3.3036	3.28	3.3046
TE_5	4.2486	4.2496	4.2499	4.2499	4.2500	4.23	-
TE_6	4.6482	4.6925	4.7022	4.7062	4.7083	4.66	-
TE_7	5.4790	5.4975	5.5004	5.5015	5.5020	-	-
TE_8	6.2840	6.2577	6.2705	6.2755	6.2781	-	-
TE_9	6.3020	6.2832	6.2832	6.2832	6.2832	-	-
TE_{10}	6.4684	6.4731	6.4748	6.4755	6.4758	-	-

Table 6. Cutoff wavenumbers of a vaned rectangular waveguide.

computed by FD-CGM is close to the cutoff wavenumber of the TM_8 or TM_9 mode computed by the multi-domain GDQ approach. Furthermore, the calculated cutoff wavenumber of the TM_6 mode by FD-CGM is close to the calculated cutoff wavenumber of the TM_{10} mode by multi-domain GDQ approach. From this comparison, it seems that the cutoff wavenumbers of some TM modes are lost in the FD-CGM computation. From the convergence trend of multi-domain GDQ results shown in Table 6, it can be seen that accurate GDQ results can be obtained by using a mesh size of 11×11. And for this case, the required computation time on LEONIS is just 7 seconds.

5. CONCLUSIONS

It is demonstrated in this paper that the multi-domain GDQ approach is very efficient for the analysis of various hollow conducting waveguides with rectangular boundaries. The present approach combines the high efficiency of the GDQ method with the flexibility of the multi-domain technique. For the analysis of double-ridged, L-shaped, single-ridged, coaxial rectangular, and vaned rectangular waveguides, it is shown that very accurate cutoff wavenumbers can be computed by multi-domain GDQ approach using very small mesh size in each subdomain. As a result, the required computation time is tiny. As the mesh size is refined, the multi-domain GDQ results will be converged to a grid-independent solution. The present approach has a potential for the analysis of complex waveguide.

REFERENCES

1. Ng, F. L., "Tabulation of methods for the numerical solution of the hollow waveguide problem," *IEEE Trans. Microwave Theory Tech.,* Vol. MTT–22, 322–329, 1974.
2. Swaminathan, M., E. Arvas, T. K. Sarkar, and A. R. Djordjevic, "Computation of cutoff wavenumbers of TE and TM modes in waveguides of arbitrary cross sections using a surface integral formulation," *IEEE Trans. Microwave Theory Tech.,* Vol. MTT–38, 154–159, 1990.
3. Sarkar, T. K., K. Athar, E. Arvas, M. Manela, and R. Lade, "Computation of the propagation characteristics of TE and TM modes in arbitrarily shaped hollow waveguides utilizing the conjugate gradient method," *J. Electromagn. Waves Appl.,* Vol. 3, 143–165, 1989.
4. Guan, J. M., and C. C. Su, "Analysis of metallic waveguides with rectangular boundaries by using the finite-difference method and the simultaneous iteration with the Chebyshev acceleration," *IEEE Trans. Microwave Theory Tech.,* Vol. MTT–43, 374–382, 1995.
5. Shu, C., "Generalized differential-integral quadrature and application to the simulation of incompressible viscous flows including parallel computation," *Ph.D. Thesis,* University of Glasgow, U. K., 1991.
6. Bellman, R., B. G. Kashef, and J. Casti, "Differential quadrature: a technique for the rapid solution of nonlinear partial differential equations," *J. Comput. Phys.,* Vol. 10, 40–52, 1972.

7. Shu, C., and B. E. Richards, "Application of generalized differential quadrature to solve two-dimensional incompressible Navier-Stokes equations," *Int. J. Numer. Methods Fluids,* Vol. 15, 791–798, 1992.
8. Shu, C., Y. T. Chew, and B. E. Richards, "Generalized differential-integral quadrature and their application to solve boundary layer equations," *Int. J. Numer. Methods Fluids,* Vol. 21, 723–733, 1995.
9. Du, H., K. M. Liew, and M. K. Lim, "Generalized differential quadrature method for buckling analysis," *Journal of Engineering, Mechanics,* Vol. 122, 95–100, 1996.
10. Shu, C., "Free vibration analysis of composite laminated conical shells by generalized differential quadrature," *J. Sound Vibr.,* Vol. 194, 587–604, 1996.
11. Montgomery, J. P., "On the complete eigenvalue solution of ridged waveguide," *IEEE Trans. Microwave Theory Tech.,* Vol. MTT–19, 547–555, 1971.
12. Utsumi, Y., "Variational analysis of ridged waveguide mode," *IEEE Trans. Microwave Theory Tech.,* Vol. MTT–33, 111–120, 1985.
13. Israel, M., and R. Miniowitz, "An efficient finite element method for nonconvex waveguide based on hermitian polynomials," *IEEE Trans. Microwave Theory Tech.,* Vol. MTT–35, 1019–1026, 1987.